

Neutral theory and scale-free neural dynamics

Matteo Martinello¹, Jorge Hidalgo¹, Serena di Santo^{2,3}, Amos Maritan¹, Dietmar Plenz⁴ and Miguel A. Muñoz^{2,*}

Abstract

Avalanches of electrochemical activity in brain networks have been empirically reported to obey scale-invariant behavior –characterized by power-law distributions up to some upper cut-off– both *in vitro* and *in vivo*. Elucidating whether such scaling laws stem from the underlying neural dynamics operating at the edge of a phase transition is a fascinating possibility, as systems poised at criticality have been argued to exhibit a number of important functional advantages. Here we employ a well-known model for neural dynamics with synaptic plasticity, to elucidate an alternative scenario in which neuronal avalanches can coexist, overlapping in time, but still remaining scale-free. Remarkably their scale-invariance does not stem from underlying criticality nor self-organization at the edge of a continuous phase transition. Instead, it emerges from the fact that perturbations to the system exhibit a neutral drift –guided by demographic fluctuations– with respect to endogenous spontaneous activity. Such a neutral dynamics –similar to the one in neutral theories of population genetics– implies marginal propagation of activity, characterized by power-law distributed causal avalanches. Importantly, our results underline the importance of considering causal information –on which neuron triggers the firing of which– to properly estimate the statistics of avalanches of neural activity. We discuss the implications of these findings both in modeling and to elucidate experimental observations, as well as its possible consequences for actual neural dynamics and information processing in actual neural networks.

Keywords

Neural avalanches — Criticality — Neutral theory — Generic scale invariance

¹ Dipartimento di Fisica ‘G. Galilei’ and CNISM, INFN, Università di Padova, Via Marzolo 8, 35131 Padova, Italy

² Departamento de Electromagnetismo y Física de la Materia e Instituto Carlos I de Física Teórica y Computacional. Universidad de Granada. E-18071, Granada, Spain.

³ Dipartimento di Fisica e Scienza della Terra, Università di Parma, via G.P. Usberti, 7/A - 43124, Parma, Italy.

⁴ Section on Critical Brain Dynamics, Laboratory of Systems Neuroscience, National Institutes of Mental Health, Bethesda, Maryland, United States of America.

*To whom correspondence should be addressed: mamunoz@onsager.ugr.es.

Introduction

The introduction by Kimura in 1968 of the neutral theory –hypothesizing that most evolutionary change is the result of genetic drift acting on neutral alleles [1]– caused much debate and a revolution in the way population genetics and molecular evolution were understood. In a similar endeavor, Hubbell proposed that most of the variability in some ecological communities could be ascribed to neutral dynamics of similar species which expand or decline as a result of stochasticity [2, 3]. Neutral theories have in common that they neglect any *a priori* intrinsic difference between coexisting individuals, regardless of their “species” (allele, tree,...) type, implying that the dynamics is purely driven by random demographic effects. For instance, the introduction of a novel species within an established population triggers a random cascade of changes, or “avalanche”, which –as a result of the implicit neutrality– does not have an inherent tendency to neither shrink nor to expand at the expenses of others. This marginal-propagation process generates scale-free avalanches, which resembles critical ones even if the system is not necessarily posed at the edge of a phase transition [3, 4] (a brief mathematical summary of neutral theory can be found in SI Appendix S1). Neutral models have been successfully employed to explain the emergence

of scale-free distributions in (i) epidemic outbreaks with neutral microbial strains [4], (ii) viral-like propagation of neutral memes [5], (iii) the evolution of the microbiome [6], and (iv) the renewal of the intestinal epithelium from neutral stem cells [7]. Could neutral theory be applied to neural dynamics of the brain? And, in particular, could it explain the emergence of neuronal avalanches reported for spontaneous activity?

The human brain has a special feature that is common to all mammals: it is endogenously active; i.e. cascades of electrochemical activity at multiple timescales spontaneously pervade its dynamical state even in the absence of any apparent stimuli or task. Mounting evidence suggests that such an endogenous activity is not random, but structured, and it contributes significantly to stimulus-related responses, being essential to brain functioning. Specifically, spontaneous, spatiotemporal bursts of neural activity were reported to appear in the form of avalanches [8], whose sizes s and durations t are distributed as $P_s(s) \sim s^{-\tau} \mathcal{F}(s/s_c)$, and $P_t(t) \sim t^{-\alpha} \mathcal{G}(t/t_c)$, respectively, where $\tau \approx 3/2$ and $\alpha \approx 2$ are critical exponents similar to those of an unbiased branching process [9, 10, 11], \mathcal{F} and \mathcal{G} are scaling functions and s_c and t_c are system-size dependent cut-offs obeying finite-size scaling [12]. Similar results have been obtained both

in vitro and *in vivo*, as well as for different tissues, preparation types, experimental techniques, and animal species (see e.g. [13, 14, 15, 16, 17, 18, 19]). Remarkably, signs of scale-invariance have been reported to vanish under abnormal circumstances such as under the influence of modified pharmacological conditions, under anesthesia, or in pathological conditions [20]. We refer to [21, 22, 23, 24, 25] for overviews and discussions on the state of the art. Taken together, these observations suggest that scale-free avalanches are a generic feature of spontaneous activity in cortical tissues, suggesting that they stem from an underlying critical phenomenon (see however [26]), and this conclusion seems to back the hypothesis that biological computing systems might operate at the edge of phase transitions [27, 28, 29], providing them with optimal transmission and storage of information, exquisite sensitivity to signals, and a number of other important functional advantages [30, 31].

Scale-free distributed events or bursts of “activity” such as earthquakes, vortex avalanches in superconductors, and Barkhausen noise are common place in Nature (see e.g. [32, 33]) and are often ascribed to their underlying dynamics being poised at a critical point. The paradigm of “self-organized criticality” was developed to explain how and why natural systems could self-tune to the vicinity of critical points [32, 34, 35]; scale-free distributed avalanches turn out to be the fingerprint of critical points of a phase transitions into quiescent (or “absorbing”) states [36, 37]. Despite the success and conceptual beauty of this framework, not all scale-invariant episodes of activity can be ascribed to underlying criticality [38, 39]; for instance, power-law distributed excursion sizes and times are generated by unbiased random walks [40], self-organization to the edge of a discontinuous phase transition [41] and, as discussed above, neutral dynamics [4, 7].

In this paper we explore the possibility that empirically observed neural avalanches could be scale-free as a result of an underlying neutral dynamics –i.e. that each single event of activity is indistinguishable from others and can marginally propagate through the network– alternatively to being self-organized to the edge of a phase transition. This is, we explore whether scale-free avalanches could stem from the neutral competition for available space of activity generated from different sources or stimuli. We put forward a subtle but important difference between such causal avalanches and existing empirical evidence, and discuss how neutral patterns of activity –i.e. coexisting causal avalanches of many different shapes, sizes and durations– could be exploited by real neural systems for efficient coding, optimal transmission of information and, thus, for memory and learning [42].

Results

Computational model and its phenomenology

Using a model of leaky integrate-and-fire neurons regulated by synaptic plasticity, Millman, *et al.* [43] were able to capture the empirical observation of bistability in cortical networks,

i.e. two well differentiated stable patterns of cortical activity, called Up and Down states (see e.g. [44, 45] and Refs. therein). Briefly, the model consists of N leaky integrate-and-fire excitatory neurons forming a directed random Erdős-Rényi network with average connectivity K . Neurons integrate synaptic inputs from other neurons and fire action potentials, which rapidly deplete associated synaptic resources. These latest recover at a slow time scale, thereby regulating the overall level of activity in the network (see MM). The model can be tuned by controlling e.g. its average synaptic strength. For weak synaptic strengths, a quiescent phase with very low levels of activity, the Down state, exists, whereas a second, stable state with high firing rates, the Up state, emerges for large synaptic strengths (see Fig. 1A). For intermediate strengths, spontaneous fluctuations allow for rapid Up and Down states alternations (see Fig. 1B). This phenomenology – which can also be reproduced by keeping synaptic strength fixed and varying the synaptic recovery time or some other parameter of the model– corresponds to a discontinuous phase transition (see Fig. 1 and Fig. 1 in [43]) and therefore lacks the critical point characteristic of continuous transitions. Remarkably, when tracking cascades of neuronal firing based on participating neurons, i.e. causal avalanches (see below), the model was shown to exhibit scale-free distributions of sizes and durations during Up-states, with associated exponents $\tau \approx 3/2$ and $\alpha \approx 2$, i.e. the hallmark of actual neuronal avalanches. Accordingly, the authors considered the Up state as “self-organized critical”, in contrast to the Down state which was “subcritical” with causal cascades that were not scale-free [43]. Given that critical dynamics emerge at continuous phase-transitions, the presence of scale-invariant Up state avalanches in the absence of any such transition in this model is puzzling, and prompted us to identify possible alternative mechanisms for the emergence of scale-free avalanches.

“Causal” avalanches

Following [43], we tracked causal cascades/avalanches.¹ Each one is initiated when an external input depolarizes a neuron’s membrane potential above its threshold to fire an action potential, it unfolds as the membrane potential of a subsequent neuron surpasses its threshold as a result of a synaptic input from an existing cascade member, and stops when this does not happen. The size of a cascade is the total number of action potentials it triggered, while the cascade duration is the timespan between its initiation and the time of its last action potential [43]. Avalanches were analyzed separately for Up and Down states in a network with $N = 3000$ neurons, using different values of the external firing rate, f_e ; in particular we analyzed the slow driving limit $f_e \rightarrow 0$. Our results are in perfect agreement with the phenomenology found in [43]: cascades in the Down state do not exhibit scale invariance but instead have a characteristic scale (see SI Appendix S2). In contrast, cascades during Up-states distribute in size and duration according to power-laws with exponent close to $\tau = 3/2$

¹Here, we use indistinctly the terms “avalanche” and “cascade”.

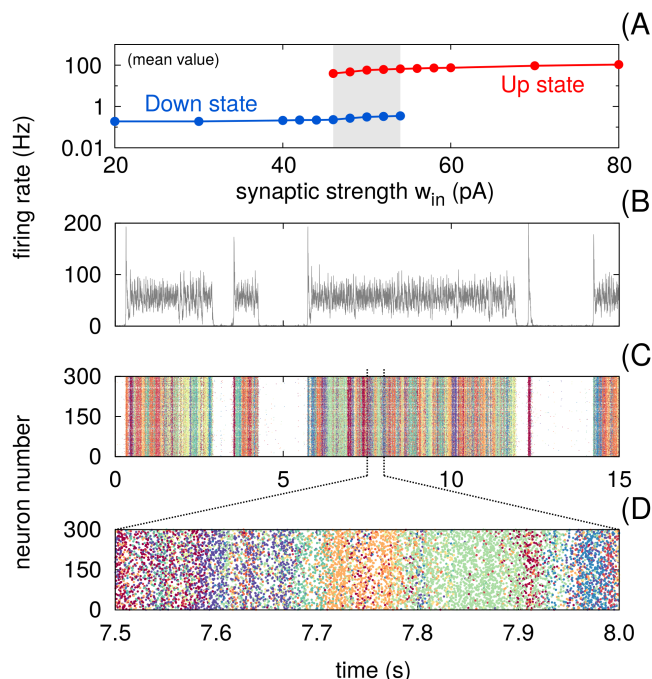


Figure 1. (Color online) Numerical integration of the model of Millman *et al.* [43] with $N = 300$ neurons. (A) Phase diagram of the mean firing rate as a function of the synaptic strength parameter, w_{in} . For low values of w_{in} , the stable state is a quiescent state with very low levels of activity (Down state), whereas for large values of w_{in} , the system exhibits high levels of activity (Up state). Both states coexist for intermediate strength values (shaded region), allowing for Up-and-Down transitions. Importantly, the transition is discontinuous. (B) Timeseries of the network firing rate for $w_{in} = 50$ pA illustrate the system’s bistability, with eventual (stochastic) jumps between Up and Down states. (C) Raster plot (for the same times as above) in which distinct colors are used for different causal avalanches, defined as subsequently activated neurons after a spontaneous activation of a neuron by an external input [43]. (D) Raster plot zoom (broken lines) demonstrating the intermingled and temporally overlapping organization of different causal avalanches. Model parameters have been set as in [43] (see MM).

and $\alpha = 2$, respectively (see Fig. 2A). As already observed in [43], these results are quite robust, do not depend on how deep into the Up state –i.e. how far from the transition point– simulations are run, nor do they change upon introducing inhibitory neurons (see SI Appendix S3).

“Time-correlated” avalanches from time binning

A key point of the previous analysis is that causal information between activation events (i.e. “who triggers who”) is essential to define avalanches. However, in empirical analyses it is not clear whether events occurring nearby in time –usually ascribed to the same avalanche in statistical analyses– are actually causally connected or not. The standard approach,

that has been successfully used in the analysis of experimental data, where causal information of event propagation is typically not accessible [8, 13], consists in defining cascades from a series of discrete supra-threshold events, by choosing a discrete time bin Δt . An avalanche is defined as a sequence of successive time windows with at least one event in each that is preceded and ended by an empty bin. In principle, one could expect different scaling relations when varying the time window Δt , as was demonstrated in analyses of empirical data [8]. For comparison, and following [8, 13], we take Δt to be equal to the average inter-event interval (IEI), defined as the average time interval between successive events.² Using this binning procedure in timeseries from the computational model, we find that cascade duration and size distributions obtained from Up states are exponentially distributed with a characteristic scale, showing no signs of scale-invariant behavior (see Fig. 2B). Distributions did not change qualitatively for different values of Δt . Thus, in the model of Millman *et al.*, cascades based on temporal proximity differ significantly from cascades based on causal information. This finding is in contrast to the established scale-free avalanche distributions that emerge from experimental data based on temporal proximity.

In the model of Millman *et al.*, causal avalanches can (and do) coexist in time (see Fig. 1C and D); thus, the temporal proximity approach does necessarily fail to uncover true causal avalanches. Thus, our observations, together with the lack of a continuous phase transition, question the origin of true scale invariance within Up states and its actual relationship with experimental findings. To shed light on this problem, in the next section we analyze a minimal model which captures the main ingredients for activity propagation, showing that the observed scale-free causal avalanches in the model of Millman *et al.* stems from an underlying neutral dynamics [4, 7].

Neutral (causal) avalanches in a minimal model for activity propagation

In archetypical models of activity propagation such as the contact process, directed percolation and the susceptible-infected-susceptible model [10, 46], “active” sites propagate activity to their nearest neighbors or become de-activated at some rates. As a result, depending on rate values, there exist a quiescent and an active phase, as well as a critical point separating them [10, 46]; avalanches started from a single initial event exhibit scale invariance only at criticality (see SI Appendix S4), and if they are triggered at a sufficiently slow rate, they do not overlap.

In contrast, within the framework of neutral dynamics, multiple avalanches can propagate simultaneously. The difference between critical and neutral avalanches can be vividly

²Even though the IEIs can vary for different experimental situations, size and duration distributions have been claimed to exhibit universal behavior with exponent $\tau \approx 3/2$ and $\alpha \approx 2$, respectively, provided that data are binned using the IEI.

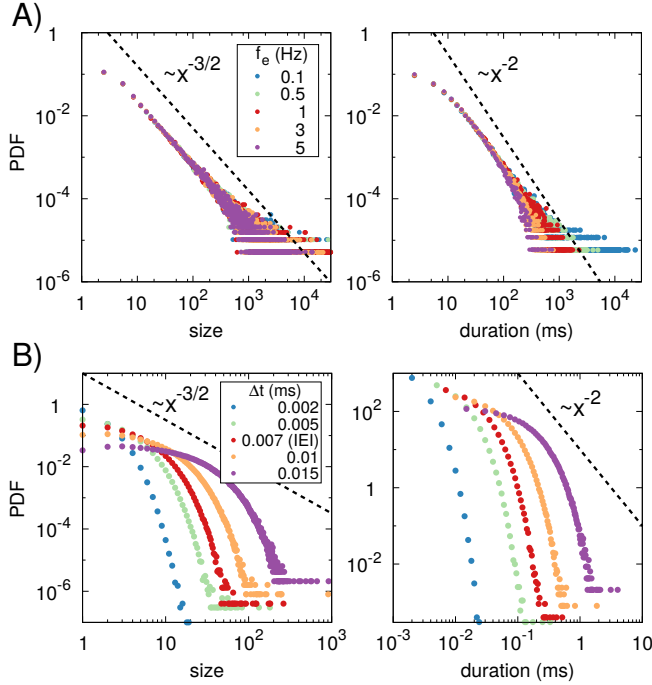
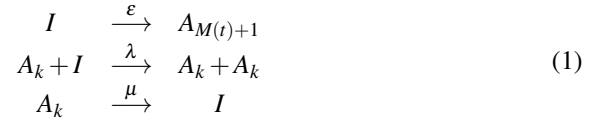


Figure 2. (Color online) Avalanche size and duration distributions within the Up-state phase in the model of Millman *et al.* [43] using two different methods (double logarithmic plot). (A) Causal avalanches were defined using the same criterion as in [43], for several values of the external input f_e , confirming the observation that sizes and durations are power-law distributed with the same exponents of an unbiased branching process, i.e. $\tau = 3/2$ and $\alpha = 2$, respectively [9, 11]. (B) “Time-correlated” avalanches, defined with the standard temporal binning method [8] (which estimates causality by temporal proximity), using five different time intervals Δt to bin the data, including one coinciding with the average interevent interval (IEI) as usually done in the analyses of empirical data [8], for $f_e = 5$ Hz; in this case distributions do not obey a power-law distribution but have a characteristic scale. In all cases, simulations were performed in a network of $N = 3000$ neurons (model parameters as in [43], see MM section).

illustrated by considering a variant of the contact process, consisting of many different but equivalent “species”. It can be studied arbitrarily far from the phase transition to explore the statistics of causal avalanches. More specifically, we consider a fully-connected network with N nodes that can be either active (A) or inactive (I). At every time, each single active site is assigned to a unique individual avalanche/species k (the one from which it derives) and labeled by A_k . The dynamics is as follows: i) a new avalanche, with a new label, is initiated by the spontaneous activation of an inactive site at small driving rate ε ; ii) active sites propagate the activity to neighboring inactive places at rate λ , and iii) active sites become inactive at rate μ . This is equivalent to the following set of reactions

for $k = 1, \dots, M(t)$:



where $M(t)$ is the total number of avalanches triggered up to time t . This dynamical process is *neutral* (or symmetrical) among avalanches/species as parameter rates do not depend on label k (see SI Appendix S1 for an extended discussion on neutral theories). The duration (resp. size) of an avalanche k is the time elapsed (resp. total number of activations) between its spontaneous generation and the extinction of its label. Observe that different avalanches can coexist (all the most in the active phase) and that the total number of coexisting avalanches can vary in time. The state of the system is determined by $M(t)$ and the number of k -type active sites, $n_k(t)$, or, equivalently, the corresponding density $\rho_k(t) = n_k(t)/N$. The total density of active sites is defined as $\rho(t) = \sum_{k=1}^{M(t)} \rho_k(t)$. Importantly, the system of Eq. (1) is nothing but the standard contact process (with a non-vanishing rate for spontaneous activation ε) if avalanche labels are ignored. Therefore, in the limit $\varepsilon \rightarrow 0$, it exhibits a continuous phase transition for the total activity density at the critical point given by $\lambda_c = \mu$ [10, 46].

We performed computer simulations of the dynamics described by Eq. (1) by means of the Gillespie algorithm [47] in a fully-connected network of size $N = 10^4$. Parameter values are chosen for the system to lie well inside the active phase, $\lambda = 2$, $\mu = 1$ (i.e. $\lambda = 2\lambda_c$), and ε taking small values such as $10^{-1}, 10^{-2}, 10^{-3}$ and 10^{-4} . Typical timeseries for individual avalanches, ρ_k , as well as for the total activity, ρ , are depicted in Fig. 3A. Observe that the steady-state overall density (gray color) coincides, on average, with that of the contact process in the infinite size limit, $\rho^* \simeq (1 - \mu/\lambda) + \varepsilon\mu/(\lambda(\lambda - \mu))$ (see MM). On the other hand, individual avalanches (colored curves in Fig. 3A) experience wild fluctuations as a function of time. The statistics of avalanches is illustrated in Fig. 3B revealing that avalanche sizes and durations are power-law distributed with exponents $\tau = 3/2$ and $\alpha = 2$ in the limit of small spontaneous activation rate $\varepsilon \rightarrow 0$. Remarkably, scale-free avalanches appear all across the active phase, $\lambda > \lambda_c$ (see SI Appendix S4).

Analytical approach

To shed light on this result, we study analytically this simplified model in the large network-size limit. Starting from the master equation associated to Eq. (1), performing a system-size expansion for large but finite system sizes [48], the dynamics of a just-created avalanche is well-described by the following equation:

$$\dot{\rho}_k = (\lambda(1 - \rho) - \mu)\rho_k + \sqrt{\frac{1}{N}(\lambda(1 - \rho) + \mu)\rho_k} \xi_k(t), \quad (2)$$

with the initial condition $\rho_k = 1/N$, and where $\xi_k(t)$ represents a zero-mean Gaussian white noise of unit variance (to

be interpreted in the Itô sense [48]). If the system is very large, and *when the spreading rate lies within the active phase* ($\lambda > \mu$), the total activity density exhibits very small fluctuations, remaining quite stable around the steady-state value, as illustrated by the gray-colored timeseries in Fig. 3A.

To understand this variability, let us assume $\rho(t) \simeq \rho^*$ in Eq. (2) and $\rho_k \ll \rho$ (which is good approximation for large system sizes where many avalanches coexist); thus,

$$\dot{\rho}_k = -\frac{\mu}{\lambda - \mu} \varepsilon \rho_k + \sqrt{\frac{\mu}{N} \left(2 - \frac{\varepsilon}{\lambda - \mu}\right)} \rho_k \xi_k(t). \quad (3)$$

In the limit of small driving, $\varepsilon \rightarrow 0$, the deterministic/drift term in Eq. (3) vanishes, and the dynamics of avalanche k can be simply written as:

$$\dot{\rho}_k = \sqrt{\rho_k} \xi_k(\hat{t}), \quad (4)$$

where for simplicity in the notation, a factor $2\mu/N$ has been reabsorbed into the time scale \hat{t} . Eq. (4) represents a freely-moving random-walk with demographic fluctuations, and—as further discussed in SI Appendix S1—it describes the evolution of a species density in any neutral-type of dynamics. In other words, once an avalanche starts, its statistics is entirely driven by neutral demographic fluctuations, *regardless of the distance to the critical point*³. Furthermore, the avalanche exponents associated with this neutral, noise-driven, dynamics are $\alpha = 2$ and $\tau = 3/2$. Actually, the previous reasoning holds all across the active (Up) phase; on the other hand, in the quiescent (Down) state, the steady state activity ρ^* goes to 0, as the deterministic driving force in Eq. (2) is negative, leading to subcritical avalanches, as indeed reported in [43].

Thus, a simple approach allowed us to explicitly show that neutral dynamics among coexisting dynamically-indistinguishable fluctuations leads to scale-free distributions all across the active (Up) phase, i.e. arbitrarily far away from the edge of the phase transition. The same conclusion extends to the model of Millman *et al.* even if detailed analytical calculations for such a case are more difficult to perform.

Discussion

A remarkable observation—that has elicited a great deal of interest—is that neural activity in the brain of mammals, including humans, occurs in the form of neuronal avalanches consisting of outbursts of neural activity intervened by periods of relative quiescence, across many resolution scales in a robust way [8, 21]. For *in vitro* studies of relatively small networks it seems plausible to assume that events occurring during one of such outbursts are causally connected, so that activity emerges at some location and transiently propagates through the network, causing a cascade of co-activations. However, there is no clear empirical validation that this is actually the case; diverse causally-connected cascades could, in principle, occur

³Not surprisingly, Eq. (4) corresponds also to the mean-field description of an unbiased branching process [9].

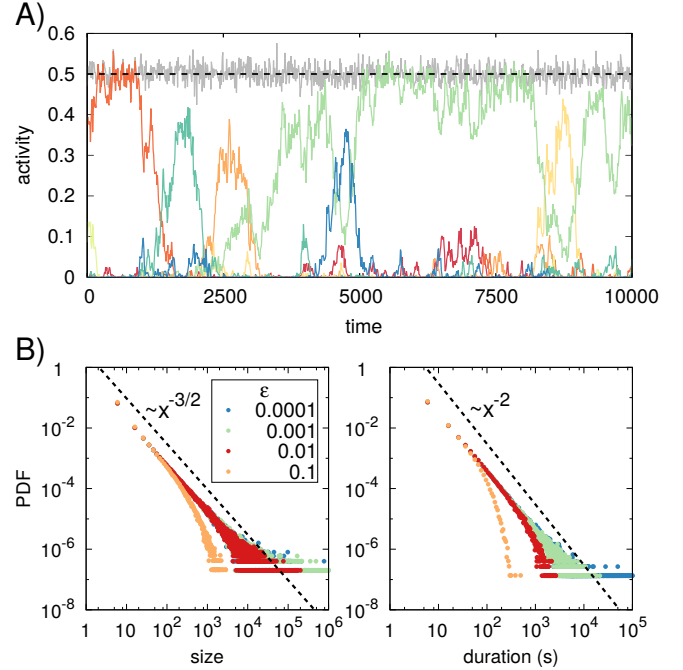


Figure 3. (Color online) Causal avalanches in a minimal model for propagation activity, defined as cascades of events initiated from the spontaneous activation of one unit, without overlap between avalanches (i.e. a given node cannot be simultaneously part of more than one avalanche). (A) The activity of each avalanche is defined as the density of active elements in the system belonging to that avalanche, identified with different colors in the plot. The global activity density is represented with the gray-colored line. Parameters of the model are taken deep inside the active phase, $\lambda = 2$, $\mu = 1$, for a system size $N = 10^4$ and small spontaneous activation rate $\varepsilon = 10^{-3}$. Whereas the global activity exhibits slight fluctuations around its steady-state value $\rho^* \simeq 1 - \mu/\lambda$ (represented by the dashed line), individual avalanches can exhibit wild variability. (B) Avalanche size and duration distributions for different values of ε (other parameters as in (A), i.e. deep inside the active phase). Avalanche statistics exhibit robust power-law scaling with the same exponents of the neutral theory for avalanche propagation (marked with dashed lines for comparison).

simultaneously, hindering their experimental discrimination as individual avalanches. Obviously, the situation is much more involved in large neural networks as analyzed *in vivo* as diverse scales of resolution, e.g. from local field potential measurements, magneto-encephalography, functional magnetic resonance imaging, etc. There is no known empirical procedure to actually disentangle causal influences, nor to discern whether different causal cascades of activations overlap (as they probably do in functional brains). Thus, in the absence of a better indicator, events of activity are customarily clustered together as individual avalanches, relying on a criterion of temporal proximity.

It thus remains to be fully elucidated what is the true nature of scale-free avalanches in actual neural systems. To shed light on this, here we scrutinized the most commonly referred model—introduced by Millman and coauthors [43]—justifying the emergence of power-law distributed avalanches in networks of integrate-and-fire neurons with synaptic plasticity. First of all, we reproduced the findings in [43], and confirmed that the model exhibits two different phases in parameter space, an Up-state characterized by large average firing rates and a Down-one with small firing, separated by a discontinuous phase transition. We carefully analyzed the dynamics within the active phase, and corroborated that diverse avalanches can coexist, and that their sizes and durations are scale-free (with exponents, $3/2$ and 2 , respectively) if and only if precise information on which neuron triggers the firing of which—which is accessible in computational models—is used to identify (causal) avalanches. On the other hand, a different analysis—which is the one customarily applied to empirical data—based on defining avalanches through a time-binning procedure, blind to detailed causal information between activation events, does not reveal any trace of scale-freedom in avalanche distributions.

These observations naturally pose two important questions. First, if this model is not self-organized to the edge of a phase transition, where do the computationally-reported scale-free (causal) avalanches within this model stem from? And second, does this model constitute a faithful representation of actual neural dynamics, including the experimentally observed scale-invariant avalanches?

To answer the first question we designed a simplified dynamical model with an overall phenomenology very similar to that of the model of [43]: i.e. it exhibits scale-invariant causal avalanches all along its active phase, regardless of the distance to a phase-transition point (which actually can be either a continuous or a discontinuous one depending on model details). This simplified model—a variant of the contact process with many different types of active particles—allowed us to uncover that scale-invariant avalanches within the active phase stem from the neutral dynamics among diverse coexisting (causal) avalanches. In particular, if new seeds of activity are injected at a very slow rate in a system with recurrent background activity (i.e. in its active phase) each one does not have a net drift toward contracting or expanding in the background of recurrent activity in which it unfolds; its dynamics just follows demographic fluctuations, much as in neutral theories of population genetics. Moreover, the branching ratio is equal to unity, and causal avalanches are power-law distributed (as in the unbiased branching processes) without the model being posed at the edge of a phase transition. In summary, the observed scale-invariance in a well-accepted computational model for neuronal dynamics as well as in a simplified model stems from the neutrality or symmetry between diverse competing cascades of causally-related events which coexists in a background of recurrent activity.

In what respects the second question above, it might occur

that the discussed computational model does not reproduce all the phenomenology of actual neural dynamics in real networks. For instance, activity exhibits clear temporal clustering (so that measured power-laws disappear when times are reshuffled [8]) and, as we have shown, this fact is mostly lacking in the model of Millman *et al.*. This drawback was overcome in a more recent and detailed computational model including many additional neuro-physiologically realistic ingredients (such as e.g. inhibitory plasticity) which exhibits temporal clustering of activity together with scale-free avalanches [49]. In this case, avalanches are also measured employing causal information so that scale-invariance is likely to stem from underlying neutrality, rather than criticality. It would be highly desirable to have a study of purely time-binned avalanches in this type of approach, allowing to compare them with causal ones. From a broader perspective, more complete computational models and/or analyses allowing to scrutinize the possible emergence and interplay between neutrality and criticality are highly needed.

Finally, the main question that remains to be answered is: given that various types of functional advantages are ascribed to criticality, do these same advantages still exist if neuronal scale-free avalanches turn out to be the consequence of underlying neutrality rather than of the tuning to the edge of a phase transition? While we do not have a definite answer to this, we speculate that this type of power-law distributed coexisting causal avalanches could play a fundamental role in neural functioning. In particular, there are known biological mechanisms, such as learning rules, that take into account causal information (i.e. which neuron triggers the firing of which); a well-documented example is “synaptic timing dependent plasticity” (STDP) [42] by which synaptic weights are either reinforced or weakened depending on the relative spike timing between the pre- and post-synaptic neuron. STDP has been found to stabilize the dynamics of neural networks and to maintain reproducible patterns of causal neuronal avalanches [49]. Thus, patterns of activity, generated by neutral dynamics, and consisting on mostly-non-interacting scale-free avalanches could be stored and stabilized or “ingrained” by such a mechanism, allowing the network to spontaneously generate a large set of attractors and a broad dynamical repertoire, in a similar way in which cellular diversity—stemming from underlying neutral dynamic of stem cells—entails functional advantages in epithelial tissues [7]. These speculative ideas need to be much more carefully scrutinized, and we plan to do so in forthcoming work.

Summing up, some of the existing confusion surrounding different types of scale-invariance in neural activity can be rationalized in the framework of neutral theories, posing new and fascinating questions that may contribute to clarify the criticality hypothesis in the cortex and its implications for function and learning.

Materials and Methods

Model for neural dynamics

The model of Millman *et al.* [43] consists of a population of N leaky integrate-and-fire excitatory neurons which are randomly connected in a directed graph to, on average, other K neurons in the population (i.e. forming a Erdős-Rényi network [50]). External inputs, $I_{in}^k(t)$, are Poisson-distributed with rate f_e and internal inputs, $I_{in}^k(t)$, are generated from spiking neurons in the network (k accounts for the input number). Both internal and external currents are modeled by exponentials functions of amplitude $w_{e/in}$ and characteristic time τ_s , $I_{in}^k(t) = w_{e/in} \exp(-(t - t_{s_i}^k)/\tau_s)$, where $t_{s_i}^k$ represents the corresponding spiking time of neuron i . Each individual neuron i is described by a dynamical variable V_i representing its membrane potential. When this value reaches a threshold value θ , the neuron spikes and it may open –with probability p_r – each of its n_r associated release sites per synapse, inducing a postsynaptic current. After spiking, the membrane potential is reset to the resting potential value, V_r , for a refractory period τ_{rp} , during which its dynamics is switched-off. Synaptic depression is implemented by means of a dynamical “utility” variable $U_{ij}(t) \in [0, 1]$ (for neuron i and release site j), which modulates the release probability $p_r \rightarrow U_{ij} p_r$. The membrane potential obeys the following equation:

$$\dot{V}_i = -\frac{V_i - V_r}{RC} + \sum_k \frac{I_{in}^k(t)}{C} + \frac{1}{C} \sum_{i' \in n.n.(i)} \sum_{j,k} \Theta(p_r U_{i'j}(t_{s_{i'}}^k) - \zeta_{i'j}^k) I_{in_{i'}}^k(t), \quad (5)$$

where R is the membrane resistance C its capacitance, k is the spike number, i' runs over presynaptic neurons linking to i , and j' over its release sites; $\zeta_{i'j}^k$ is a uniform random number in $[0, 1]$ and $\Theta(x)$ the Heaviside step function. On the other hand, the synaptic utility U_{ij} is set to 0 immediately after a release and recovers exponentially to 1 at constant rate, τ_R :

$$\dot{U}_{ij} = \frac{1 - U_{ij}}{\tau_R} - \sum_k U_{ij} \Theta(p_r - \zeta_{ij}^k) \delta(t - t_{s_i}^k). \quad (6)$$

As equations (5) and (6) are linear during successive events, they can be integrated exactly, which allowed us to implement both synchronous (or clock-driven) and asynchronous (or event driven) methods [51], leading to essentially indistinguishable results. When not specified, model parameters were taken as in [43]: $K = 7.5$, $n_r = 6$, $R = 2/3$ G Ω , $C = 30$ pF, $V_r = -70$ mV, $\theta = -50$ mV, $w_e = 95$ pA, $w_{in} = 50$ pA, $p_r = 0.25$, $\tau_{rp} = 1$ ms, $\tau_s = 5$ ms and $\tau_R = 0.1$ s. We also studied versions of the model including inhibitory couplings, but this did not alter the main conclusions (see SI Appendix S3).

Steady state density in the minimal model for activity propagation

Neglecting fluctuations from finite size effects, the dynamics of the total density of activity for the process described by Eq. (1) becomes deterministic in the limit $N \rightarrow \infty$: $\dot{\rho} = (\lambda(1 - \rho) - \mu)\rho + \varepsilon(1 - \rho)$. Its stationary solution, $\dot{\rho} = 0$, is $\rho^* = (\lambda - \mu - \varepsilon - \sqrt{4\varepsilon\lambda + (\lambda - \mu - \varepsilon)^2})/2\lambda$, that, up to first order in ε , can be written as $\rho^* \simeq 1 - \mu/\lambda + \varepsilon\mu/(\lambda(\lambda - \mu))$ in the active phase, $\lambda > \mu$, and $\rho^* \simeq \varepsilon/(\mu - \lambda)$ in the quiescent one, $\lambda < \mu$.

Acknowledgments

We are grateful to the Spanish-MINECO for financial support (under grant FIS2013-43201-P; FEDER funds) and to P. Villegas, P. Moretti, S. Suweis and S. Vassanelli for extremely useful discussions and comments.

References

- [1] Kimura M (1984) *The neutral theory of molecular evolution* (Cambridge University Press).
- [2] Hubbell SP (2001) *The unified neutral theory of biodiversity and biogeography (MPB-32)* (Princeton University Press) Vol. 32.
- [3] Azaele S, et al. (2016) Statistical mechanics of ecological systems: Neutral theory and beyond. *Rev. Mod. Phys.* 88:035003.
- [4] Pinto OA, Muñoz MA (2011) Quasi-neutral theory of epidemic outbreaks. *PLoS one* 6:e21946.
- [5] Gleeson JP, Ward JA, O’sullivan KP, Lee WT (2014) Competition-induced criticality in a model of meme popularity. *Physical Review Letters* 112:048701.
- [6] Zeng Q, Sukumaran J, Wu S, Rodrigo A (2015) Neutral models of microbiome evolution. *PLoS Comput Biol* 11:e1004365.
- [7] Lopez-Garcia C, Klein AM, Simons BD, Winton DJ (2010) Intestinal stem cell replacement follows a pattern of neutral drift. *Science* 330:822–825.
- [8] Beggs JM, Plenz D (2003) Neuronal avalanches in neocortical circuits. *J Neurosci* 23:11167–11177.
- [9] Harris TE (2002) *The theory of branching processes* (Courier Corporation).
- [10] Marro J, Dickman R (1999) *Nonequilibrium Phase Transition in Lattice Models* (Cambridge University Press).
- [11] Zapperi S, Lauritsen KB, Stanley HE (1995) Self-organized branching processes: mean-field theory for avalanches. *Physical review letters* 75:4071.
- [12] Binney J, Dowrick N, Fisher A, Newman M (1993) *The Theory of Critical Phenomena* (Oxford University Press, Oxford).
- [13] Petermann T, et al. (2009) Spontaneous cortical activity in awake monkeys composed of neuronal avalanches. *Proc Natl Acad Sci USA* 106:15921–15926.
- [14] Mazzoni A, et al. (2007) On the dynamics of the spontaneous activity in neuronal networks. *PLoS one* 2:e439.
- [15] Haimovici A, Tagliazucchi E, Balenzuela P, Chialvo DR (2013) Brain organization into resting state networks emerges at criticality on a model of the human connectome. *Phys. Rev. Lett* 110:178101.
- [16] Tagliazucchi E, Balenzuela P, Fraiman D, Chialvo DR (2012) Criticality in large-scale brain fmri dynamics unveiled by a novel point process analysis. *Frontiers in Physiology* 3:15.
- [17] Shriki O, et al. (2013) Neuronal avalanches in the resting MEG of the human brain. *The Journal of Neuroscience* 33:7079–7090.
- [18] Bellay T, Klaus A, Seshadri S, Plenz D (2015) Irregular spiking of pyramidal neurons organizes as scale-invariant neuronal avalanches in the awake state. *ELife* 4:e07224.
- [19] Poil SS, Hardstone R, Mansvelder HD, Linkenkaer-Hansen K (2012) Critical-state dynamics of avalanches and oscillations jointly emerge from balanced excitation/inhibition in neuronal networks. *The Journal of Neuroscience* 32:9817–9823.

- [20] Massobrio P, de Arcangelis L, Pasquale V, Jensen HJ, Plenz D (2015) Criticality as a signature of healthy neural systems. *Criticality as a signature of healthy neural systems: multi-scale experimental and computational studies* p 4.
- [21] Schuster HG, Plenz D, Niebur E (2014) *Criticality in neural systems* (John Wiley & Sons).
- [22] Chialvo DR (2010) Emergent complex neural dynamics. *Nature Phys* 6:744–750.
- [23] Plenz D (2012) Neuronal avalanches and coherence potentials. *The European Physical Journal Special Topics* 205:259–301.
- [24] Beggs JM (2008) The criticality hypothesis: How local cortical networks might optimize information processing. *Phil Trans R Soc A* 366:329–343.
- [25] De Arcangelis L, Lombardi F, Herrmann H (2014) Criticality in the brain. *Journal of Statistical Mechanics: Theory and Experiment* 2014:P03026.
- [26] Touboul J, Destexhe A (2010) Can power-law scaling and neuronal avalanches arise from stochastic dynamics? *PloS one* 5:e8982.
- [27] Langton C (1990) Computation at the edge of chaos: Phase transitions and emergent computation. *Physica D: Nonlinear Phenomena* 42:12–37.
- [28] Bertschinger N, Natschläger T (2004) Real-time computation at the edge of chaos in recurrent neural networks. *Neural Computation* 16:1413–1436.
- [29] Hidalgo J, et al. (2014) Information-based fitness and the emergence of criticality in living systems. *Proceedings of the National Academy of Sciences* 111:10095–10100.
- [30] Shew WL, Plenz D (2013) The functional benefits of criticality in the cortex. *The Neuroscientist* 19:88–100.
- [31] Kinouchi O, Copelli M (2006) Optimal dynamical range of excitable networks at criticality. *Nature Physics* 2:348–351.
- [32] Bak P (1996) *How nature works: the science of self-organized criticality* (Copernicus New York).
- [33] Sethna JP, Dahmen KA, Myers CR (2001) Crackling noise. *Nature* 410:242–250.
- [34] Jensen HJ (1998) *Self-organized criticality: emergent complex behavior in physical and biological systems* (Cambridge university press).
- [35] Pruessner G (2012) *Self-organised criticality: theory, models and characterisation* (Cambridge University Press).
- [36] Dickman R, Muñoz MA, Vespignani A, Zapperi S (2000) Paths to self-organized criticality. *Brazilian Journal of Physics* 30:27–41.
- [37] Bonachela JA, Muñoz MA (2009) Self-organization without conservation: true or just apparent scale-invariance? *J. Stat. Mech.* p P09009.
- [38] Grinstein G (1995) in *Scale invariance, interfaces, and non-equilibrium dynamics* (Springer), pp 261–293.
- [39] Newman MEJ (2005) Power laws, Pareto distributions and Zipf’s law. *Contemp Phys* 46:323–351.
- [40] Krapivsky PL, Redner S, Ben-Naim E (2010) *A kinetic view of statistical physics* (Cambridge University Press).
- [41] di Santo S, Burioni R, Vezzani A, Muñoz MA (2016) Self-organized bistability associated with first-order phase transitions. *Physical Review Letters* 116:240601.
- [42] Abbott LF, Nelson SB (2000) Synaptic plasticity: taming the beast. *Nature neuroscience* 3:1178–1183.
- [43] Millman D, Mihalas S, Kirkwood A, Niebur E (2010) Self-organized criticality occurs in non-conservative neuronal networks during ‘up’ states. *Nat. Phys.* 6:801–805.
- [44] Steriade M, Timofeev I (2003) Neuronal plasticity in thalamocortical networks during sleep and waking oscillations. *Neuron* 37:563–576.
- [45] Hidalgo J, Seoane L, Cortes J, Muñoz M (2012) Stochastic amplification of fluctuations in cortical upstates. *PLoS One* 7(8):e40710.
- [46] Henkel M, Hinrichsen H, Lübeck S (2008) *Non-equilibrium Phase Transitions: Absorbing phase transitions*, Theoretical and mathematical physics (Springer, Berlin).
- [47] Gillespie DT (1977) Exact stochastic simulation of coupled chemical reactions. *The journal of physical chemistry* 81:2340–2361.
- [48] Gardiner C (2009) *Stochastic Methods: A Handbook for the Natural and Social Sciences*, Springer Series in Synergetics (Springer).
- [49] Stepp N, Plenz D, Srinivasa N (2015) Synaptic plasticity enables adaptive self-tuning critical networks. *PLoS computational biology* 11.
- [50] Newman MEJ (2003) The structure and function of complex networks. *SIAM Review* 45:167–256.
- [51] Brette R, et al. (2007) Simulation of networks of spiking neurons: a review of tools and strategies. *Journal of computational neuroscience* 23:349–398.

Supporting Information:

Neutral theory and scale-free neural dynamics

M. Martinello, J. Hidalgo, S. di Santo, A. Maritan, D. Plenz and M. A. Muñoz*

*E-mail: mamunoz@onsager.ugr.es

SI Appendix S1: Brief summary of neutral theory

Consider a fully connected network with N nodes (extensions to regular lattices, or more complex networks architectures are also possible, but we stick here to the simplest case) and a number of possible states (be these species, alleles, opinions, etc.). Each node adopts one of the possible states at every time. The dynamics proceeds as follows: at each time step, one randomly chosen individual is “invaded” by a copy of another neighboring node at uniform rate, i.e. common to all the individuals in the population independently of their species labels. Without loss of generality, we focus in the dynamics of a particular species, that we call A , and consider that any other individuals corresponds to species B , i.e. for simplicity we consider the case with just two species. This is nothing but the “voter model” (VM) [1, 2, 3, 4], also known as Moran process in the context of population dynamics and population genetics (see e.g. [5]). The VM has been profusely studied in the mathematical literature; some of its main relevant features are [1, 2, 3, 4, 5]: (i) it has no free parameters, (ii) it lacks any characteristic (length or time) scale and its dynamics exhibits scale-invariance, and (iii) it is characterized by purely noise-driven diffusive dynamics (see [3, 4] for more mathematical in-depth presentations).

Now, we derive the coarse-grained mean-field description of a voter model; similar derivations can be found in the literature [5]. For the sake of illustration, let us consider also a general model in which λ_A (resp. λ_B) is the probability for A (resp. B) to invade a site in state B (resp. A), with $\lambda_A \neq \lambda_B$ in general; the VM dynamics is recovered imposing the neutral condition $\lambda_A = \lambda_B$.

As the system is saturated, the number of individuals for the other species is $n_B = N - n_A$ and the state of the system can be determined by the total number of individuals of A , n_A . The model can be expressed as a branching process [1], with transition rates $W(n_A \rightarrow n_A + 1) = \lambda_A n_B n_A / N$ and $W(n_A \rightarrow n_A - 1) = \lambda_B n_A n_B / N$. Using these rates, writing down the master equation for the probability of finding the system in a state n_A at time t –or alternatively with a density of individuals A , $\rho_A = n_A / N$ – and performing a standard large N expansion, one readily obtains the following Fokker-Planck equation:

$$\frac{\partial P(\rho_A, t)}{\partial t} = -(\lambda_A - \lambda_B) \frac{\partial}{\partial \rho_A} [\rho_A(1 - \rho_A)P(\rho_A, t)] + \frac{\lambda_A + \lambda_B}{2N} \frac{\partial^2}{\partial \rho_A^2} [\rho_A(1 - \rho_A)P(\rho_A, t)], \quad (\text{S1})$$

or its equivalent (Itô) Langevin equation

$$\dot{\rho}_A = (\lambda_A - \lambda_B)\rho_A(1 - \rho_A) + \sqrt{\frac{\lambda_A + \lambda_B}{N}\rho_A(1 - \rho_A)}\eta(t), \quad (\text{S2})$$

where η is a zero-mean Gaussian white noise with $\langle \eta(t)\eta(t') \rangle = \delta(t - t')$.

The neutrality condition $\lambda_A = \lambda_B$ implies that the deterministic drift in Eq. (S2) vanishes thus $\langle \dot{\rho}_A \rangle = 0$, i.e. the average density of each species remains constant on average; their populations do not grow nor shrink on average, but they experience stochastic demographic changes as described by

$$\dot{\rho}_A = \sqrt{\rho_A(1 - \rho_A)}\eta(\tilde{t}) \quad (\text{S3})$$

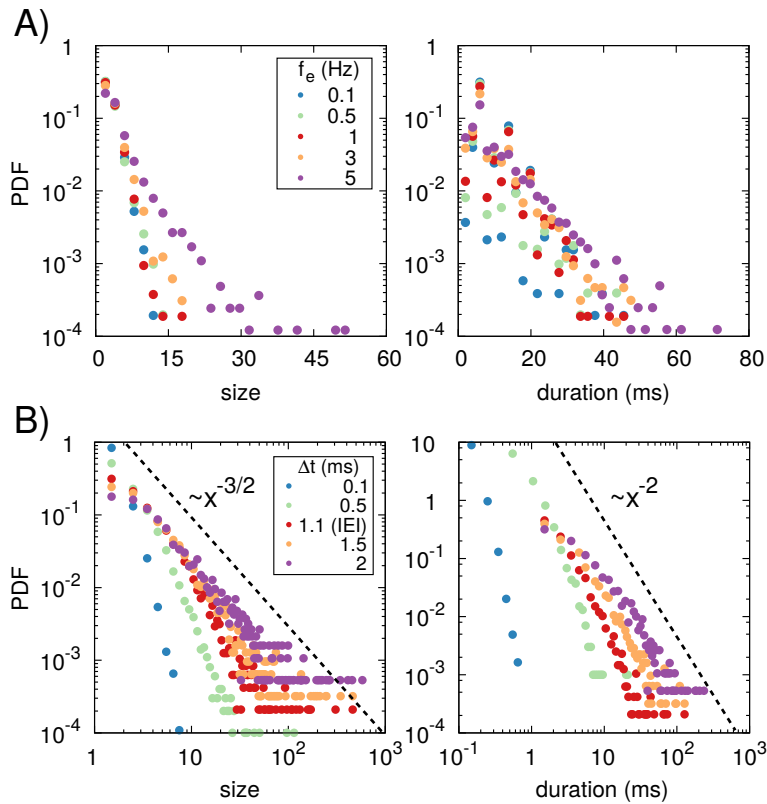
where a factor $2\lambda_A/N$ has been absorbed into the new timescale \tilde{t} .

Observe that this last equation describes a stochastic process (random walk) with two absorbing barriers at 0 and 1. By neglecting the quadratic term in the noise (which is a valid approximation as far as the avalanche is small with respect to the much-larger system size), the avalanche-time exponent $\alpha = 2$ can be

deduced from the first-passage time (return to the origin) statistics of this random-walk process, and using simple scaling arguments one can also easily derive $\tau = 3/2$ for the avalanche-size distribution [6], i.e. one recovers the mean-field exponents of the voter model (neutral theory) class (see e.g. [7]). Needless to say that these same exponent values can also be computed by employing the more standard generating function formalism for a critical branching process (see, e.g. [1, 8]).

A difference between the VM dynamics and the contact-process-like one described in the main text is that in the VM the system is “saturated”, in the sense that each single site is in one of the two possible opinions/alleles/species/labels/states, whereas in the model we study, some sites can be inactive, not belonging to any avalanche. However, looking at the dynamics of individual avalanches, such a difference becomes irrelevant.

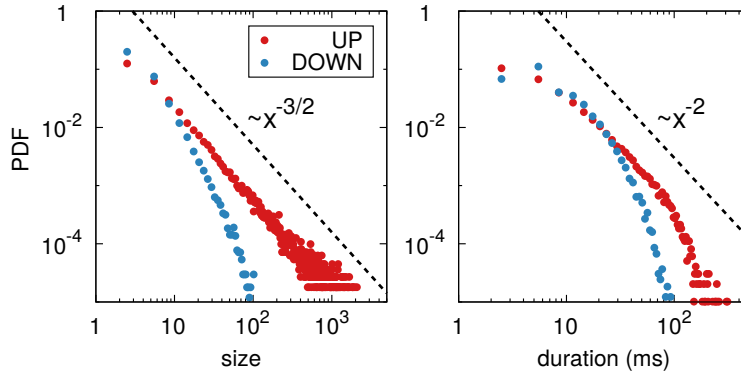
SI Appendix S2: Avalanche statistics for Down states in the model of Millman *et al.*



Supplementary Figure S1: Avalanche size and duration distributions relative to periods of low activity (Down states) for timeseries generated with the model of Millman *et al.* [9] using two different methods. Panel A (linear-logarithmic plot): “Causal” avalanches were defined using the same criterion as in [9], for several values of the external input f_e , confirming the observation that sizes and durations are exponentially distributed. Panel B (double logarithmic scale): “Time-correlated” avalanches, defined with the standard temporal binning method [10] (which ignores causal information), using five different time intervals Δt to bin the data, including one coinciding with the average interevent interval (IEI) as usually done in the analyses of empirical data [10], for $f_e = 5$ Hz. In all cases, simulations were performed in a network of $N = 3000$ neurons (model parameters as in [9], see MM in main text).

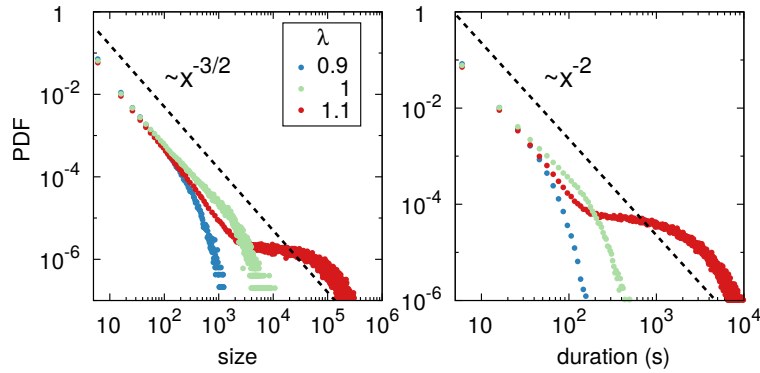
SI Appendix S3: Causal avalanches in the model with inhibitory synapses

Results presented in the main text are robust under the introduction of inhibitory synapses. Following [9], we run simulations of the model for which 20% of the neurons are initialized as inhibitory (so their output current has amplitude $-w_{\text{inh}}$) and, to keep the network balanced, each single neuron receives $k_i = k = 10$ inputs, 2 of which are from inhibitory ones. The introducing of inhibitory currents increases the coefficient of variation of spiking times, leading to enhanced variability. Still, as above, there exists a wide region of the parameter space, within the Up state (active phase) where causal avalanches keep showing scale-invariant behavior (see Fig. S2). More specifically, this happens whenever the amplitude of the inhibitory current is not too strong (so as to allow for the Up state to exist) and for values of the inhibitory synaptic timescale up to four times larger than the excitatory one.

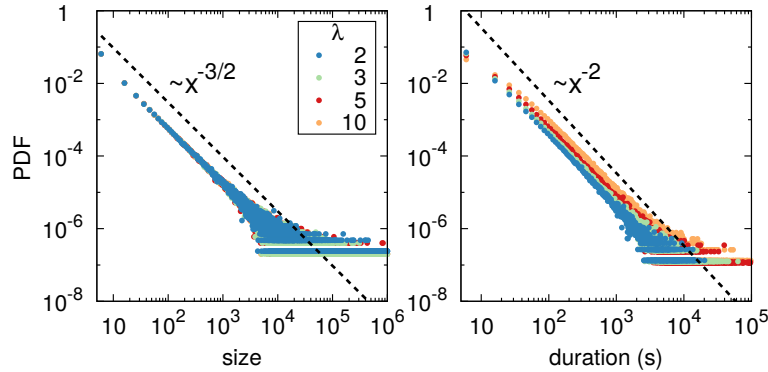


Supplementary Figure S2: “Causal” avalanche size (Left) and duration (Right) distributions in the model of Millman *et al.* including inhibitory synapses. The avalanche statistics exhibit a robust power-law scaling with the same exponents of a critical branching process (marked with dashed lines for comparison) with the Up state, while they are exponentials, with a characteristic scale in the Down state. Simulations were performed in a network of $N = 3000$ neurons setting the inhibition amplitude to $w_{\text{inh}} = 50$ pA, and other parameters as in [9] (see MM in main text).

SI Appendix S4: Avalanche statistics in the simplified model



Supplementary Figure S3: Avalanche size (Right) and duration (Left) distributions in the simplified model for activity propagation when avalanches propagate in the network one at a time, i.e. without overlap between avalanches. This is done by setting $\epsilon = 0$ and introducing one single active node each time the activity stops. Distributions are plotted for different values of the activation rate λ in the quiescent phase ($\lambda = 0.9$), active phase ($\lambda = 1.1$) and at criticality ($\lambda = 1$), illustrating the PDFs are not scale-invariant, except right at the critical point. Parameter values are: $\mu = 1$, $N = 10^3$.



Supplementary Figure S4: “Causal” avalanche size (Right) and duration (Left) distributions in the simplified model for activity propagation when multiple avalanches coexist in the network, for different values of the activation rate λ along the active (UP) phase (corresponding to stationary densities around $\rho^* = 0.5, 0.66, 0.8$ and 0.9 , respectively). In all cases, avalanche statistics exhibit a robust power-law scaling with the same exponents of a critical branching process (marked with dashed lines for comparison). Increasing the spreading rate results in an enlargement of the mean duration of avalanches, with negligible effect on the size distributions. Parameter values are: $\mu = 1$, $\epsilon = 10^{-3}$, $N = 10^4$.

References

- [1] Harris TE (2002) *The theory of branching processes* (Courier Corporation).
- [2] Marro J, Dickman R (1999) *Nonequilibrium Phase Transition in Lattice Models* (Cambridge University Press).
- [3] Dornic I, Chaté H, Chave J, Hinrichsen H (2001) Critical coarsening without surface tension: The universality class of the voter model. *Physical Review Letters* 87:045701.

- [4] Al Hammal O, Chaté H, Dornic I, Muñoz MA (2005) Langevin description of critical phenomena with two symmetric absorbing states. *Physical review letters* 94:230601.
- [5] Blythe RA, McKane AJ (2007) Stochastic models of evolution in genetics, ecology and linguistics. *Journal of Statistical Mechanics: Theory and Experiment* 2007:P07018.
- [6] di Santo S, Villegas P, Burioni R, Muñoz MA (2017) Simple unified view of branching process statistics: Random walks in balanced logarithmic potentials. *Phys. Rev. E* 95:032115.
- [7] Pinto OA, Muñoz MA (2011) Quasi-neutral theory of epidemic outbreaks. *PloS one* 6:e21946.
- [8] Zapperi S, Lauritsen KB, Stanley HE (1995) Self-organized branching processes: mean-field theory for avalanches. *Physical review letters* 75:4071.
- [9] Millman D, Mihalas S, Kirkwood A, Niebur E (2010) Self-organized criticality occurs in non-conservative neuronal networks during ‘up’ states. *Nat. Phys.* 6:801–805.
- [10] Beggs JM, Plenz D (2003) Neuronal avalanches in neocortical circuits. *J Neurosci* 23:11167–11177.